PHYSICS OF FLUIDS **25**, 095102 (2013)

A novel forcing technique to simulate turbulent mixing in a decaying scalar field

Phares L. Carroll,[1,a)] Siddhartha Verma,[2,b)] and G. Blanquart[1,c)]
[1]*Department of Mechanical Engineering, California Institute of Technology, Pasadena, California 91125, USA*
[2]*Graduate Aerospace Laboratories, California Institute of Technology, Pasadena, California 91125, USA*

(Received 12 February 2013; accepted 16 August 2013; published online 6 September 2013)

To realize the full potential of Direct Numerical Simulation in turbulent mixing studies, it is necessary to develop numerical schemes capable of sustaining the flow physics of turbulent scalar quantities. In this work, a new scalar field forcing technique, termed "linear scalar forcing," is presented and evaluated for passive scalars. It is compared to both the well-known mean scalar gradient forcing technique and a low waveshell spectral forcing technique. The proposed forcing is designed to capture the physics of one-time scalar variance injection and the subsequent self-similar turbulent scalar field decay, whereas the mean scalar gradient forcing and low waveshell forcing techniques are representative of continuous scalar variance injection. The linear scalar forcing technique is examined over a range of Schmidt numbers, and the behavior of the proposed scalar forcing is analyzed using single and two-point statistics. The proposed scalar forcing technique is found to be perfectly isotropic, preserving accepted scalar field statistics (fluxes) and distributions (scalar quantity, dissipation rate). Additionally, it is found that the spectra resulting from the three scalar forcing techniques are comparable for unity Schmidt number conditions, but differences manifest at high Schmidt numbers. These disparities are reminiscent of those reported between scaling arguments suggested by theoretical predictions and experimental results for the viscous-convective subrange. © *2013 AIP Publishing LLC*. [http://dx.doi.org/10.1063/1.4819782]

I. INTRODUCTION

A passive scalar is a quantity in a flow that will convect and diffuse without impacting the evolution of the velocity field. The mixing of these types of scalars in turbulent flow environments is found in a broad range of fields, including combustion, atmospheric flow dynamics, and oceanography. Direct Numerical Simulation (DNS) studies of scalar mixing often use numerically-forced velocity and scalar fields to prevent the turbulent fluctuations from decaying. To ensure that results obtained in such DNS studies are representative of the physics of scalar mixing, and not an artifact of the numerical schemes, the forcing methods used must not alter the physics of the flow configuration to be studied. The most commonly used method for sustaining turbulent fluctuations in a scalar field is to supply scalar variance continuously via a spatially-uniform mean scalar gradient.[1,2] Spectral schemes utilizing low waveband forcing[3] have been used also, and these supply scalar variance over a narrow band of waveshells within the turbulent scalar field. These methods are both equivalent to holding the scalar variance constant via continuous variance injection. This work presents a new scalar forcing technique that instead uses one-time variance injection to prevent variance decay. It

[a)]Electronic mail: plcarroll@caltech.edu
[b)]Electronic mail: sverma@caltech.edu
[c)]Electronic mail: g.blanquart@caltech.edu

is shown that this new scalar forcing methodology corresponds to a distinctly different physics than the other two commonly used methods.

There are many applications in which forcing proportional to a scalar gradient is physically meaningful. In many oceanographic and atmospheric flows, there are gradients in species concentration or temperature. In these instances, as long as the gradient of the scalar quantity of interest is uniform over distances longer than the largest characteristic length-scale of the turbulent flow, implementing such a numerical forcing technique is entirely consistent with the physics of the flow configuration.[4] Applying a spatially uniform scalar gradient across the scalar field allows this field to remain homogeneous and to reach a state of statistical stationarity.[5] Nevertheless, the imposed mean scalar gradient introduces robust anisotropy into the scalar field, which can be problematic for studies of scalar mixing under isotropic conditions. Low waveshell spectral forcing techniques[3] eliminate this problem by implementing a perfectly isotropic forcing term. However, these schemes are less physically representative of experimentally-attainable flows.

The goal of this work is to develop and validate a new scalar field forcing technique that can capture the physics of self-similar scalar field decay, which is an inherently different physics than that captured by the two existing scalar forcing methods. The objectives for this forcing are twofold. First, the forcing must be able to reproduce scalar mixing in physically-relevant turbulent flows. Second, the forcing must preserve the statistics of isotropic turbulence across all scales of the flow. These requirements will be considered in light of existing velocity forcing methods, which have been proven to be effective means of preventing turbulent kinetic energy from decaying.[6,7] Central to this work is the observation that turbulent mixing of scalars may not always occur in an environment where the scalar field is subject to continuous energy injection. In other words, these scalars may undergo turbulent mixing where there is only an initial source of scalar energy, followed by scalar variance decay. This new proposed scheme aims to create a scalar field constrained to constant scalar energy (or scalar variance) under these conditions, and it will be shown to be equivalent to creating a state of "normalized decay." Examples of situations for which this forcing would be appropriate can be found in engineering applications, such as in heated grid turbulence experiments, and in natural phenomena, such as sedimentation processes found in oceanographic flows. This proposed forcing scheme, referred to as the linear scalar forcing throughout this paper, is validated against its ability to predict the statistical characteristics and energy spectrum of a scalar field subject to temporal decay. The forcing method is examined over a range of relatively low Taylor micro-scale Reynolds numbers (Re_λ) and low to moderately high Schmidt numbers (Sc).

The structure of this paper is as follows. Section II discusses the mean scalar gradient and low waveshell forcing techniques and their characteristics. Additionally, the linear velocity forcing technique primarily used in this study is discussed and its connection to the physics of a decaying turbulent velocity field is presented. Building on the observations made in Sec. II, Sec. III details the derivation of the proposed linear scalar forcing technique. Section IV presents the process by which the appropriateness of the proposed forcing for simulating scalar field decay is validated. Finally, Sec. V discusses the role of scalar field forcing in mixing studies at high Schmidt numbers.

II. MOTIVATION: CURRENTLY IMPLEMENTED FORCING TECHNIQUES

A. Mean scalar gradient forcing

In simulation studies of turbulent passive scalar mixing, the mean scalar gradient forcing technique superimposes a uniform mean gradient across the scalar field,

$$z = Z + \boldsymbol{G} \cdot \boldsymbol{x}, \tag{1}$$

where the total scalar quantity, z, is broken down into a fluctuating part, Z, and a spatially-varying mean part, $\boldsymbol{G} \cdot \boldsymbol{x}$. All simulations discussed in this paper impose the mean gradient in a single direction, $\boldsymbol{G} = [-1, 0, 0]$. Such a forcing technique captures the formation of ramp-cliff structures and the intermittency of the scalar field, consistent with the findings of experimental studies of passive scalar mixing, by virtue of the anisotropy it induces.[8,9] This scalar forcing technique is quite effective and was created to capture the scalar field behavior present in grid turbulence experiments.

The transport equation for the fluctuating scalar in the presence of a mean gradient, assuming incompressibility ($\nabla \cdot \boldsymbol{u} = 0$), is given by

$$\frac{\partial Z}{\partial t} + \boldsymbol{u} \cdot \nabla Z = \nabla \cdot (\mathcal{D} \nabla Z) - \boldsymbol{u} \cdot \boldsymbol{G}, \tag{2}$$

where $\mathcal{D}$ is the molecular diffusivity. The imposed mean scalar gradient term ($\boldsymbol{G}$) acts as an infinite reservoir for the scalar field; whenever there are losses due to dissipation, the presence of a gradient term will immediately "inject" into the scalar field a scalar quantity magnitude sufficient to compensate. Thus, it provides for continuous scalar energy injection, sustaining the scalar field at a statistically stationary state. Beginning with the forced advection-diffusion equation, Eq. (2), and multiplying by the scalar fluctuation, Z, results in

$$\frac{\partial \left(Z^2\right)}{\partial t} + \nabla \cdot \left(\boldsymbol{u} Z^2\right) = \nabla \cdot \left(\mathcal{D} \nabla Z^2\right) - \chi - 2\, Z\, (\boldsymbol{G} \cdot \boldsymbol{u}), \tag{3}$$

where $\chi = 2\mathcal{D} \mid \nabla Z \mid^2$ is the scalar dissipation rate and incompressibility, again, has been assumed. When Eq. (3) is averaged over a triply periodic, homogeneous domain (in which all work to be presented is conducted), only the time derivative, scalar dissipation rate, and the forcing term retain non-zero values. This leaves

$$\frac{\partial \langle Z^2 \rangle}{\partial t} = -\langle \chi \rangle - 2\, \boldsymbol{G} \cdot \langle \boldsymbol{u} Z \rangle = -\langle \chi \rangle + 2\, \langle u_x Z \rangle. \tag{4}$$

The angled brackets, $\langle \cdot \rangle$, refer to volumetric averages. Equation (4) implies that if the scalar field were to attain perfect isotropy (i.e., $\langle u_i Z \rangle = 0$), then the time-rate of change of scalar variance would always be negative and equal to the scalar dissipation rate, causing continuous scalar field decay. It is the anisotropy, evident from the skewed probability density function (PDF) of the scalar fluxes in Fig. 1, that prevents the variance of the scalar field from decaying.

Also, due to the anisotropy inherent in this forcing mechanism, it is used primarily for passive scalars; the velocity field affects the scalar field, but the scalar field does not couple back to effect the velocity field. With an active scalar, the coupling is two-way, with information being passed between the turbulent velocity and scalar fields. The anisotropy that is methodically maintained in the scalar field would have the opportunity to permeate into the velocity field. There may be physical configurations in which such a coupling is consistent with the physics governing the problem, but this may not always be the case.

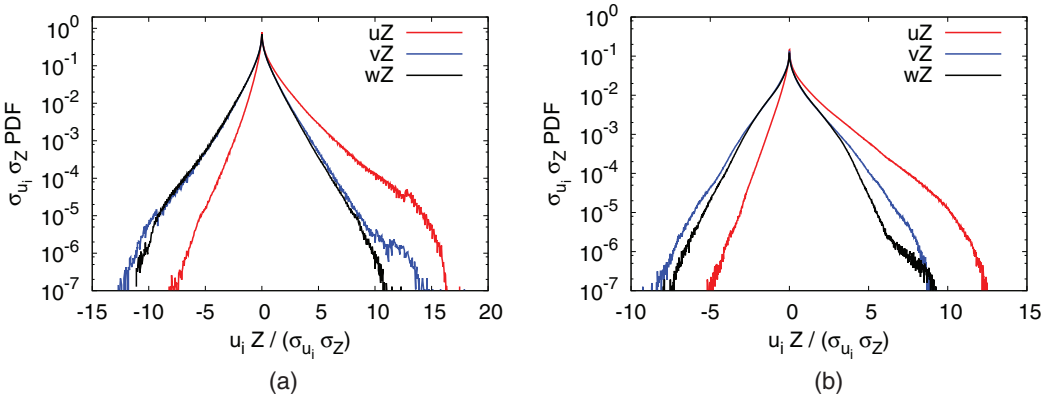

FIG. 1. PDF of scalar fluxes obtained using a mean scalar gradient forcing and two different velocity forcing techniques[7,10] ($N = 512^3$, $Re_\lambda = 140$, $Sc = 1$, $\kappa_{max}\eta_B = 1.5$). The σ variables refer to standard deviations. (a) Spectral velocity forcing;[10] (b) linear velocity forcing.[7]

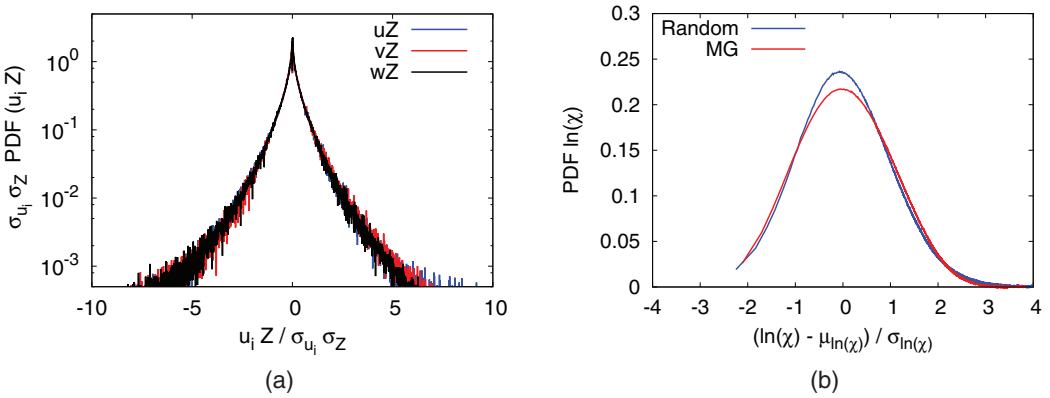

FIG. 2. Statistical metrics of the scalar field produced via low waveband spectral (random) forcing versus mean gradient forcing (MG) ($N = 256^3$, $Re_\lambda = 55$, $Sc = 1$, $\kappa_{max}\eta_B = 3.0$). (a) Scalar fluxes, u_iZ; (b) scalar dissipation rate, χ.

B. Low waveshell spectral forcing

Spectral forcing techniques continuously provide energy into the scalar field over a range of tightly constrained, low wavenumber shells ($\kappa_{lower} \leq \kappa \leq \kappa_{upper}$).[3,11,12] The advection-diffusion equation resulting from such a forcing scheme is given by

$$\frac{\partial Z}{\partial t} + \boldsymbol{u}\cdot\nabla Z = \nabla\cdot(\mathcal{D}\nabla Z) + \mathscr{F}_{\underline{x}}^{-1}\{\hat{f}_Z(\kappa)\}, \tag{5}$$

where $\mathscr{F}_{\underline{x}}^{-1}$ denotes the inverse Fourier-transform of the forcing term in spectral space. The spectral forcing implemented in this work has a forcing term with a Gaussian distribution centered about a wavenumber of $\kappa = 3$ that is active only between the upper and lower bounds of $\kappa_{upper} = 4$ and $\kappa_{lower} = 2$. With such a forcing scheme, as with the mean gradient method, the scalar variance is held fixed in time because losses from scalar dissipation are balanced by continuous injection of scalar variance into the scalar field by the forcing term, $\langle Z\mathscr{F}^{-1}{}_{\underline{x}}\{\hat{f}_Z(\kappa)\}\rangle$. The primary (and only significant) difference between mean gradient and spectral scalar forcing methods is that a random spectral forcing is capable of producing perfectly isotropic scalar fluxes, as illustrated in Fig. 2(a). The character of the scalar field produced under the action of the two forcings are consistent. Both produce a scalar quantity that is approximately normally distributed about a mean of zero and a log-normally distributed scalar dissipation rate. Representative results are provided in Fig. 2(b). Furthermore, as depicted in Fig. 3, a low waveband spectral forcing scheme and the mean scalar gradient scheme give comparable scalar spectra over a range of Sc. Representative low and high Sc cases are included in support of this claim.

As the only chief difference in these two methods is the issue of isotropy in the scalar fluxes, the rest of this paper will focus primarily on the direct comparison of the proposed linear scalar forcing method to the mean scalar gradient forcing method. This comparison was preferred, as the mean scalar gradient is more widely applied in simulation studies of mixing and the configuration it represents is more readily attainable experimentally.

C. Forcing the velocity field linearly

There are two broadly-accepted ways of forcing the velocity field in numerical studies, linearly[6,7] and spectrally.[10] The present work draws on Lundgren's linear forcing scheme[6,7] as inspiration for the development of the linear scalar forcing technique. According to the linear forcing scheme, momentum is injected into the velocity field proportional to the magnitude of the velocity fluctuations and assumes the form

$$\frac{\partial \boldsymbol{u}}{\partial t} + \boldsymbol{u}\cdot\nabla\boldsymbol{u} = -\nabla\left(\frac{p}{\rho}\right) + \nu\nabla^2\boldsymbol{u} + Q\boldsymbol{u}, \tag{6}$$

where Q is a constant related to the energy dissipation rate and eddy turn-over time, τ.

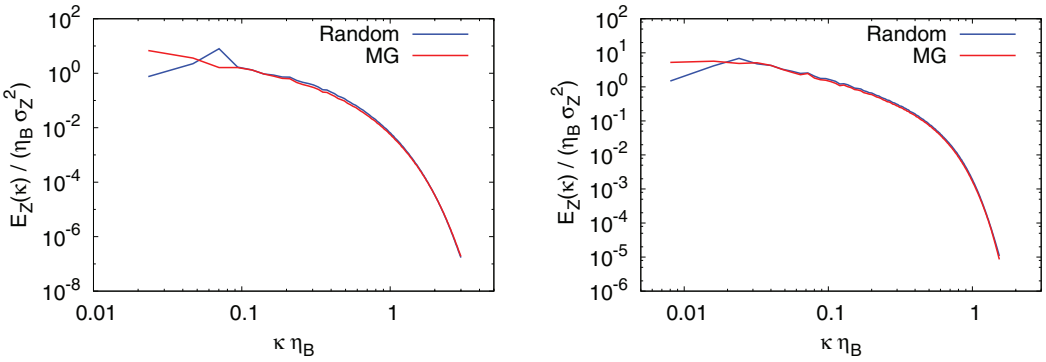

FIG. 3. Comparison of scalar energy spectra obtained using the mean gradient (MG) and random spectral forcing. (a) $N = 256^3$, $Re_\lambda = 55$, $Sc = 1$, $\kappa_{max}\eta_B = 3.0$ (linear velocity forcing[7]); (b) $N = 384^3$, $Re_\lambda = 8$, $Sc = 256$, $\kappa_{max}\eta_B = 1.5$ (spectral velocity forcing[10]).

Forcing linearly is equivalent to injecting energy at all scales of the flow, from the integral scales to the dissipative scales. But, as the fluctuations are the largest at the integral scales, the energy injection is biased preferentially towards these large scales. The linear forcing scheme was found to produce characteristics consistent with the requirements of homogeneous, isotropic turbulence, namely, equal-averaged Reynolds stresses and symmetrically distributed scalar fluxes with reflectional symmetry.[7] More relevant to the present work, Lundgren's linear forcing method can be connected directly to the self-similar nature of decaying turbulence.[6] In this method, energy injection can be thought of as a rescaling of the kinetic energy to a constant value. By performing a simple change of variables in space, time, and velocity on the forced and unforced (freely decaying) momentum equations, Lundgren[6] found that the transformed freely decaying momentum equation admitted terms that were similar in form to those present in the linearly-forced momentum equation. From this finding, he concluded that the effect of the linear forcing technique is similar to that of energy decay, which is inherently isotropic and self-similar. Thus, the self-similar decay of energy in the velocity field was suggested to be analogous to the imposed isotropic forcing term, $Q\boldsymbol{u}$.[6]

III. PROPOSED LINEAR SCALAR FORCING

A. Self-similarity of scalar mixing

Following Lundgren's[6] work on linear velocity forcing, the objective of this work is to develop a new forcing scheme that reproduces the physics of the self-similar decay of a scalar field. The self-similar regime of scalar mixing manifests itself whenever there is one-time energy injection into a scalar field. Following this energy injection, there is a short-lived transient period of decay which eventually gives way to a self-similar flow regime. Self-similarity, in the context of a decaying scalar field, is characterized by the collapse of freely decaying scalar spectra onto a single spectrum shape after appropriate normalization. To demonstrate this aspect of self-similarity, a scalar field was forced to statistical stationarity and then allowed to decay. Referring to Fig. 4(a), the scalar forcing was removed at $t/\tau = 0$, and the variance was allowed to decay. It is clear from Fig. 4(a) that the scalar field is losing variance without the forcing term active. Figure 4(b) illustrates the behavior of the self-similar field; the three normalized scalar spectra in Fig. 4(b) correspond to the three data points in Fig. 4(a) at 1, 2.7, and 6.5 τ after the scalar forcing was removed. The coincidence of the spectra to one unchanging shape when normalized by their variances (and Batchelor scales) indicates that this scalar field has entered the self-similar regime.

Considering the nature of self-similar decay, it can be argued that to model this type of scalar mixing, a scalar forcing method based on scalar energy normalization would be needed. These concepts of energy normalization and self-similarity, in addition to Lundgren's[6] insight that an

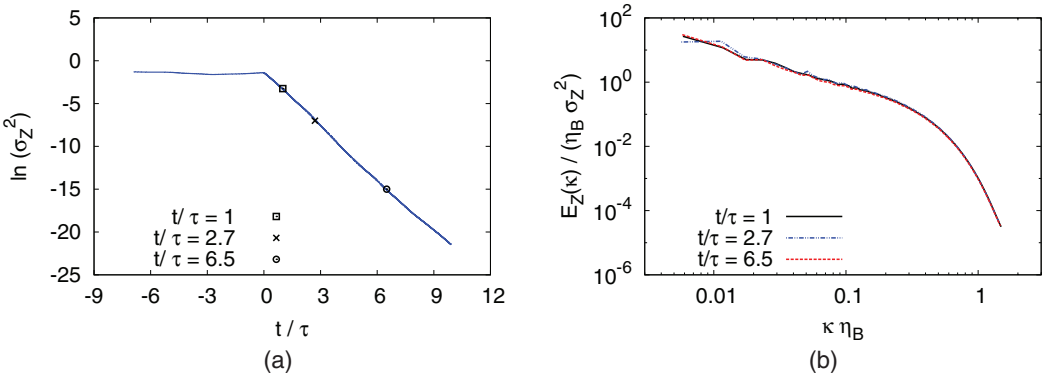

FIG. 4. Decay of scalar variance and collapse of scalar energy spectra in the self-similar regime ($N = 512^3$, $Re_\lambda = 140$, $Sc = 1$, $\kappa_{max}\eta_B = 1.5$). (a) Scalar variance; (b) normalized scalar spectra.

isotropic forcing can be thought of in terms of sustained, normalized energy decay, serve as the foundation for the development of the proposed linear scalar forcing method.

B. Derivation of the proposed linear scalar forcing term

As mentioned previously, the development of this new scalar forcing is motivated by the successful implementation[7] of the linear velocity forcing of Lundgren[6] and the concepts of normalization and self-similarity. Note that in the derivation to follow that, although the same variables are used to denote scalar quantities (Z and z), these quantities do not have the same definitions that were used in Secs. II A and II B. Following Lundgren's[6] linear velocity forcing, a normalization method is needed to drive the scalar field (z) towards a constant energy, or variance, $\sigma_z^2 = \langle z^2\rangle - \langle z\rangle^2$. After initialization, all turbulent quantities begin to decay as they are convected and diffused through the simulation domain. The proposed scalar forcing technique seeks to generate self-similar conditions by implementing two steps. First, a normalization step. Second, a step to drive the scalar field to a specified, imposed variance value, α. The absolute value of the rescaled scalar field variance (α) is inconsequential; the significant factor is solely that the scalar field variance is constant in time.

Beginning with the renormalization step, the scalar field is rescaled according to

$$Z = z\sqrt{\frac{\alpha}{\sigma_z^2}}, \tag{7}$$

where Z is the normalized, forced scalar quantity, z is the unforced (non-normalized) scalar quantity, and σ_z^2 is the variance of the non-normalized scalar field. Using the normalization defined, the required form of the linearly-forced advection-diffusion equation can be determined readily by consideration of the spatially-averaged variance equation (Eq. (4) without the mean gradient term),

$$\frac{\partial \sigma_z^2}{\partial t} = -\langle \chi \rangle, \tag{8}$$

where it has been assumed that the mean of the decaying scalar quantity is zero, $\langle z\rangle = 0$. By differentiating Eq. (7) and substituting Eq. (8), the rate of change of the rescaled scalar quantity, Z, is of the form

$$\frac{\partial Z}{\partial t} = \sqrt{\frac{\alpha}{\sigma_z^2}}\frac{\partial z}{\partial t} + \frac{1}{2}\frac{\langle \chi(z)\rangle}{\sigma_z^2}Z, \tag{9}$$

where $\langle \chi(z)\rangle$ and σ_z^2 are functions of the decaying scalar (z), not the rescaled scalar (Z). Recall the advection-diffusion equation for any scalar quantity can be expressed as

$$\frac{\partial z}{\partial t} = \nabla\cdot(\mathcal{D}\nabla z) - \boldsymbol{u}\cdot\nabla z. \tag{10}$$

Using this expression for $\frac{\partial z}{\partial t}$, Eq. (9) becomes

$$\frac{\partial Z}{\partial t} = \frac{1}{2}\frac{\langle \chi(z)\rangle}{\sigma_z^2} Z + \frac{\sqrt{\alpha}}{\sigma_z}\left(\nabla\cdot(\mathcal{D}\nabla z) - \boldsymbol{u}\cdot\nabla z\right). \tag{11}$$

Note that α and σ_z^2 are volume-averaged quantities and are, therefore, constant with respect to any spatial derivative. In other words,

$$\nabla Z = \frac{\sqrt{\alpha}}{\sigma_z}\nabla z \tag{12}$$

$$\Rightarrow \chi\,(Z) = \chi\,(z)\,\frac{\alpha}{\sigma_z^2}. \tag{13}$$

Substituting these expressions into Eq. (11) results in an expression for the time-rate of change of the rescaled scalar quantity in terms of Z only,

$$\frac{\partial Z}{\partial t} = \nabla\cdot(\mathcal{D}\nabla Z) - \boldsymbol{u}\cdot\nabla Z + \frac{1}{2}\frac{\langle\chi(Z)\rangle}{\alpha} Z. \tag{14}$$

Although the above expression is mathematically consistent with the rescaling step, it was found that the scalar field could become divergent, depending on its initial variance. It is the presence of α in the denominator that is responsible for this behavior. This behavior can be understood by examining the variance equation corresponding to Eq. (14). Upon volume-averaging, applying the condition of homogeneity, and recalling the definition of χ, Eq. (15) is obtained:

$$\frac{\partial\langle Z^2\rangle}{\partial t} = \frac{\partial\langle\sigma_Z^2\rangle}{\partial t} = \langle\chi(Z)\rangle\left(\frac{\sigma_Z^2}{\alpha} - 1\right). \tag{15}$$

By inspection of Eq. (15), if the variance value (σ_Z^2) is less than (greater than) α, then the time derivative of scalar variance will attain a negative (positive) value, and the scalar variance will decay away towards zero (grow indefinitely).

To avoid this problem, an approximation is made. As it is the long-time scalar field behavior with which this study is interested, not the initial transient behavior, α was replaced with the variance of the rescaled scalar field, σ_Z^2. This is a justifiable approximation, as at stationarity, the rescaled scalar field variance will approach α. This is not the case in the initial transient period, but it is true in the long-time limit, $\alpha = \sigma_Z^2$. Thus, Eq. (14) can be written as

$$\frac{\partial Z}{\partial t} = \nabla\cdot(\mathcal{D}\nabla Z) - \boldsymbol{u}\cdot\nabla Z + \frac{1}{2}\frac{\langle\chi(Z)\rangle}{\sigma_Z^2} Z. \tag{16}$$

With such an expression, the right-hand side of Eq. (15) now becomes zero, enabling the scalar field to attain a state of constant variance.

C. Compensating for discretization errors and controlling the scalar field variance

The solution of the above equation analytically would lead to a statistically stationary scalar field with a constant variance, as the newly added production term would balance exactly all molecular dissipation. Assuming the scalar transport scheme implemented in the numerical solver is energy conserving, this production term is sufficient to produce a scalar field with a constant time-averaged variance. However, if the transport scheme implemented is not energy conserving (e.g., Weighted-Essentially Non-Oscillatory (WENO),[13] High-Order Upwind Convective (HOUC),[14] or Quadratic Upstream Interpolation for Convective Kinematics (QUICK)[15] schemes), then there will be losses in scalar variance due to numerical diffusion. These losses can be easily compensated for via the addition of a second term, which is active only when the effects of numerical diffusion manifest in the scalar field.

The constraints in constructing this second term are threefold. First, it should take the form of a relaxation term, being active only when the variance of the rescaled scalar field is not equal to α. This will have the effect of driving the variance to α and sustaining it at α, providing the user with

control over the final, stationary scalar field variance value. This control over the variance of the scalar field, combined with knowledge of the mean of the scalar field, gives the user the ability to define completely the statistical distribution of the scalar quantity of interest. This statement will be supported further in Sec. IV C. Second, it needs to be dimensionally consistent with Eq. (14) (or Eq. (16)). Finally, the additional term should be linear with respect to the rescaled scalar quantity, such that it preserves the linearity of the rescaled and unforced advection-diffusion equations. In light of these requirements, this additional relaxation term is of the form

$$\frac{1}{\tau_R}\left(\sqrt{\frac{\alpha}{\sigma_Z^2}}-1\right)Z, \tag{17}$$

where τ_R is a relaxation time-scale. If $\sigma_Z^2=\alpha$, then the term is inactive, as the variance of the rescaled field is at its desired value; if $\sigma_Z^2\neq\alpha$, then more (or less) variance is added to (or subtracted from) the rescaled scalar field. The role of the relaxation time-scale is to prevent the relaxation term from adjusting too strongly to changes in scalar variance. Using a time-scale associated with the larger scale flow structures instead of a smaller time-scale on the order of viscous processes (where losses in scalar variance actually occur) ensures that the scalar variance is adjusted sufficiently slowly and smoothly to prevent transient behaviors from being introduced in the scalar field. As an example, the value of α can be chosen to match exactly the variance of the initial scalar field. However, this is not a requirement.

The final form of the scalar transport equation with the proposed linear scalar forcing technique is obtained by combining Eqs. (16) and (17),

$$\frac{\partial Z}{\partial t}+\boldsymbol{u}\cdot\nabla Z=\nabla\cdot(\mathcal{D}\nabla Z)+\left[\frac{1}{\tau_R}\left(\sqrt{\frac{\alpha}{\sigma_Z^2}}-1\right)+\frac{1}{2}\frac{\langle\chi(Z)\rangle}{\sigma_Z^2}\right]Z. \tag{18}$$

To reiterate, the proposed forcing function is composed of two terms; the relaxation term allows the scalar field to evolve towards a specified variance, or average scalar energy, while the production term balances exactly any losses from scalar dissipation. Note, however, that the relaxation term is required only if the scalar transport scheme used is not energy conserving; if it is energy conserving, then the relaxation term will be effectively inactive. This proposed linear scalar forcing scheme has the advantage of being truly mathematically isotropic, imposing no preferred direction. It is interesting to note that the production term is similar to the linear velocity forcing term, $Q\boldsymbol{u}$. Analogous to Q, the linear factor,

$$\frac{1}{2}\frac{\langle\chi(Z)\rangle}{\sigma_Z^2},$$

is the inverse of a time-scale. However, in this case, it is the inverse of the scalar time-scale, $\tau_Z=\sigma_Z^2/\chi(Z)$.

IV. VALIDATION OF THE VARIANCE FORCING TECHNIQUE

The validation of the proposed linear scalar forcing takes the following form. First, the temporal behavior of the forcing is investigated to ensure the average scalar variance asymptotes indeed to a constant value, independent of the initial conditions. Second, the impact of varying the magnitude of the relaxation time-scale is studied. Third, the relevant single-point metrics for isotropy, such as skewness, variance, and the three scalar fluxes, are calculated to ensure appropriate behavior. Additionally, the distributions of scalar quantities with accepted analytical forms, such as the distribution of the scalar dissipation rate (log-normal), are calculated and verified to be predicted correctly. Finally, two-point statistics (e.g., spectra) are considered. For each (Re_λ,Sc) combination included in this study, the spectra generated from the linear scalar forcing are compared to spectra from the decay of a scalar field in the self-similar regime.

TABLE I. Simulation parameters for the DNS study conducted. N is the number of grid points, and $\mathcal{D}$ is the molecular diffusivity of the scalar quantity.

Variation of Schmidt number Fixed: HOUC5 scheme (except case 4), $\tau_R = 1$						
Case ID	N^3	Re_λ	$\kappa_{max}\eta$	$\kappa_{max}\eta_B$	Sc	$\mathcal{D}$
1	256^3	55	3.0	3.0	1	7.50×10^{-3}
2	256^3	55	2.4	3.4	0.5	1.50×10^{-2}
3[a]	1024^3	55	11.8	2.95	16	4.69×10^{-4}
4[a,b,c]	1024^3	140	3.4	3.4	1	2.80×10^{-3}
5[b]	768^3	8	49	3.06	256	6.20×10^{-4}
Variation of scalar transport scheme Fixed: $\tau_R = 1$, $Sc = 1$, $Re_\lambda = 55$						
Case ID	N^3	Re_λ	$\mathcal{D}$	$\kappa_{max}\eta_B$	Scalar scheme	
1	256^3	55	7.50×10^{-3}	3.0	HOUC5	
6	256^3	55	7.50×10^{-3}	3.0	QUICK	
Variation of relaxation timescale Fixed: HOUC5 scheme, $Sc = 1$, $Re_\lambda = 55$						
Case ID	N^3	Re_λ	$\mathcal{D}$	$\kappa_{max}\eta_B$	τ_R	
1	256^3	55	7.50×10^{-3}	3.0	1	
7	256^3	55	7.50×10^{-3}	3.0	0.1	
8	256^3	55	7.50×10^{-3}	3.0	0.5	
Variation of initial condition Fixed: HOUC5 scheme, $\tau_R = 1$, $Sc = 1$, $Re_\lambda = 55$						
Case ID	N^3	Re_λ	$\mathcal{D}$	$\kappa_{max}\eta_B$	Initial condition	
9	256^3	55	7.50×10^{-3}	3.0	Gaussian	
10	256^3	55	7.50×10^{-3}	3.0	Random	
11	256^3	55	7.50×10^{-3}	3.0	Mean scalar gradient-forced	

[a]For these cases, $\tau_R = 0.1$. This was done to reduce computational burden for this Re_λ, Sc combination.
[b]For these cases, the velocity field was spectrally-forced;[10] all others were linearly-forced.
[c]For this case, the QUICK scalar transport scheme was used.

A. Simulation study

The primary objective of this study is to evaluate the characteristics of the proposed linear scalar forcing technique in homogeneous, isotropic turbulent flow over a range of Schmidt numbers. The velocity field is linearly forced[7] in cases 1–3 and cases 6–11 (Table I), as discussed in Sec. II C, and spectrally forced[10] in cases 4–5 to maintain a suitable Re_λ. The scalar field is forced with both the proposed method (referred to as linear scalar (LS)) and the mean scalar gradient method (referred to as MG) to allow for comparison.

The specific simulation parameters and fluid properties (kinematic viscosity, $\nu = \mathcal{D}\,Sc$, and molecular diffusivity, $\mathcal{D}$), are summarized in Table I. The columns titled $\kappa_{max}\eta$ and $\kappa_{max}\eta_B$ are indicative of the simulation resolution, where κ_{max} corresponds to the maximum wavenumber accessible in the simulation, η is the Kolmogorov length-scale, and η_B is the Batchelor[19] length-scale, defined as $\eta_B = \eta Sc^{-\frac{1}{2}}$. The Kolmogorov and Batchelor[19] length-scales indicate the smallest characteristic length-scales for the velocity and scalar fields, respectively. Convention mandates highly restrictive resolution requirements for both the velocity and scalar fields when performing DNS studies, or the physics of the dynamically important small scales will not be captured fully. The accepted resolution limits for the velocity and scalar fields are $\kappa_{max}\eta \geq 1.5$ and $\kappa_{max}\eta_B \geq 1.5$, respectively,[16] for spectral codes. As the code package implemented in this work is non-spectral, the limits $\kappa_{max}\eta \geq 3.0$ and $\kappa_{max}\eta_B \geq 3.0$ will be used. One unfortunate result of these resolution criteria is that simulation studies are restricted to moderate Schmidt numbers, as high-Schmidt number simulations can become too computationally expensive to perform.

To illustrate the robustness and validity of the proposed scalar forcing, a parametric study was performed. The parameters methodically varied include the relaxation time-scale, τ_R, the scalar

transport scheme, the nature of the initial conditions, and the Schmidt number, Sc. As will become evident in Secs. IV B–IV D, the proposed linear scalar forcing is quite robust.

The simulations to be presented were conducted in a configuration of 3D periodic turbulence of size $(2\pi)^3$. They were performed with the NGA code package.[17] The code is physical (non-spectral) and uses a standard staggered grid. The velocity field is solved implicitly via a second-order accurate finite-difference scheme, and this scheme is energy conserving. The scalar field is solved implicitly via either the QUICK scalar transport scheme, which is a third-order upwinded finite-volume scheme,[15] or a fifth-order accurate upwinded scheme (HOUC5).[14] The time advancement is accomplished via a semi-implicit Crank-Nicolson method.[17]

B. Time evolution

To illustrate the effectiveness of the proposed scalar forcing at driving the scalar field towards a state of constant variance, consider Fig. 5(a), which contains the evolution of variance of the scalar field as a function of time for cases 1–3 in Table I. Initially, the energy content of the scalar field is negligible. As the forcing is applied, the field assumes progressively a constant scalar variance value, as determined by the value of α specified. For all simulations performed, α was set to unity. As can be verified from Fig. 5(a), the energy content of the scalar field does relax towards a constant value.

However, depending on the quality of the scalar transport scheme used, the scalar variance may not assume a value of precisely unity. This is illustrated in Fig. 5(b). The disparity can be explained as follows. The third-order accurate QUICK scheme suffers from comparatively greater numerical diffusion than the fifth-order accurate HOUC5 scheme. Both curves shown in Fig. 5(b) were obtained using the same value of τ_R, which is not sufficient to overcome the effects of numerical diffusion when the QUICK scheme is used for scalar transport. Upon decreasing the value of τ_R, the steady state scalar variance obtained with the QUICK scheme increased towards the desired value. Note that the highest $Re_\lambda = 140$ case included in this study was run with the QUICK transport scheme instead of the less dissipative HOUC5 scheme due to numerical stability issues. To compensate for any losses from utilizing the QUICK scheme, this $Re_\lambda = 140$ case was run at a very high resolution, $\kappa\eta_B = 3.4$.

These observations verify that both the production and relaxation terms are necessary for the success of the proposed scalar forcing technique. The production term compensates for losses in scalar variance from physical diffusion, and the relaxation term accommodates for errors in the scalar transport scheme and determines the final, steady state variance value. Further evidence of the need to compensate for discretization errors can be obtained by examining Fig. 6, which depicts

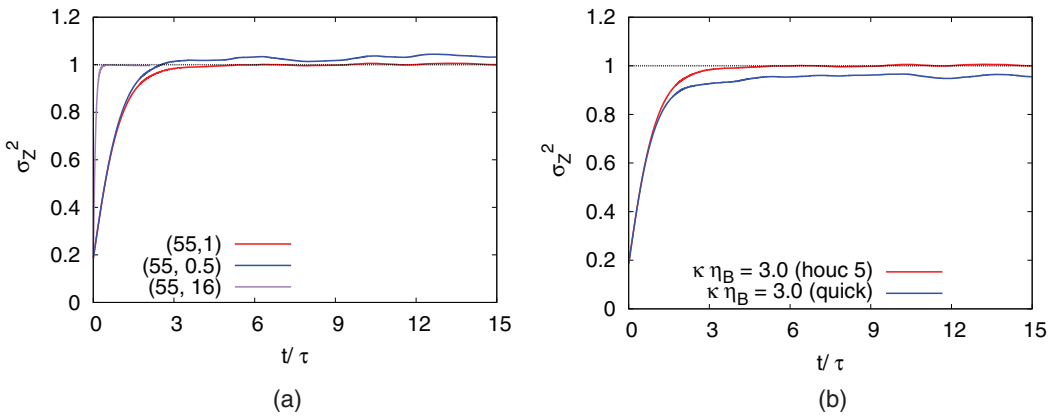

FIG. 5. Time evolution of scalar field statistics for $\alpha = 1$. (a) Time evolution of scalar field variance. $Re_\lambda = 55$, $Sc = 16$ plateaus more quickly as $\tau_R = 0.1$. The legend refers to (Re_λ, Sc); (b) effect of reducing numerical error via improving the scalar scheme (cases 1 and 6, $Re_\lambda = 55, Sc = 1$).

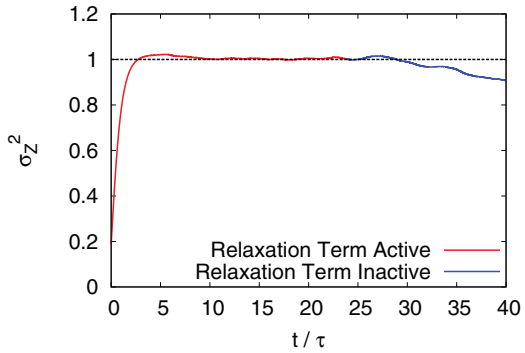

FIG. 6. Effect of relaxation term on scalar field variance $Re_\lambda = 55$, $Sc = 1$, $\kappa\eta_B = 3.0$. Note that the scalar field variance is unchanged from that of the initial scalar field for 5τ when the relaxation term is zeroed.

the temporal variance data obtained when the proposed linear scalar forcing is run with and without the relaxation term active. Initially ($t/\tau \leq 23$), the relaxation term is active and the scalar variance is driven to and sustained at the specified $\alpha = 1$ value. Then, the relaxation term is removed from the forcing ($t/\tau \geq 23$). The scalar variance is observed to remain constant for approximately 5 τ before losses due to the imperfect nature of the HOUC5 scheme begin to manifest as a reduction in variance. Assuming perfect energy conservation in the scalar transport scheme, the production term would be sufficient to sustain the scalar field at the desired variance value. Unfortunately, no scalar transport scheme is truly energy conserving; physical schemes induce discretization errors and spectral schemes may induce dealiasing errors. As a result, the relaxation term is necessary, and once at statistical stationarity, it is only needed to compensate for numerical errors.

Recall that τ_R (the relaxation parameter) is a free parameter which controls the overall stiffness of the forced scalar transport equation, Eq. (18). To show the effectiveness of the proposed scheme at driving the scalar field towards stationarity, τ_R is varied, as indicated in cases 1, 7, and 8. Figure 7(a) indicates the impact of the relaxation parameter on the performance of the proposed forcing. A smaller value, $\tau_R = 0.1$, results in a faster initial rise to the specified variance and serves to weight the relaxation term preferentially in comparison to the production term.

Further, the behavior of this linear scalar forcing is independent of initial conditions. The effect of the initial conditions was qualified by making use of three different initialization methods. First, the initial scalar field was generated as Gaussian in space (case 9), following the scalar field initialization technique of Eswaran and Pope.[18] Second, a completely random field was used to

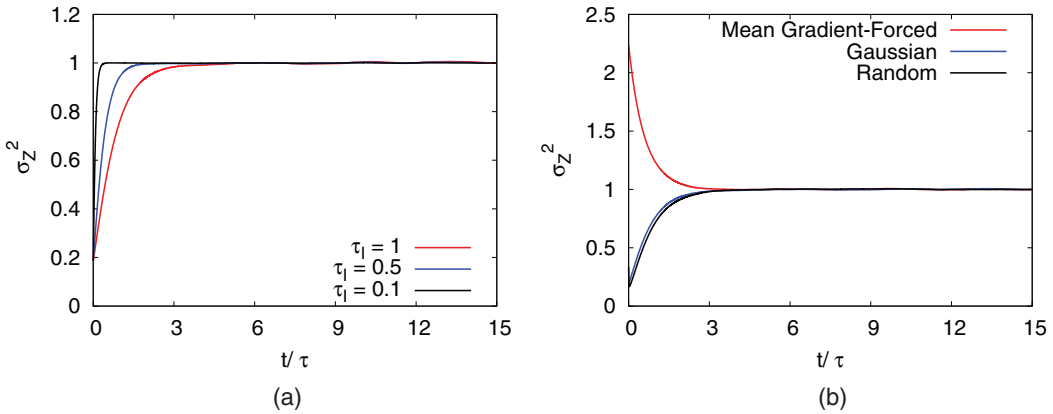

FIG. 7. Effect of relaxation time-scale and initial conditions on the performance of the proposed linear scalar forcing ($Re_\lambda = 55, Sc = 1$). (a) Effect of the relaxation time-scale ($\kappa_{max}\eta_B = 3.0$, cases 1, 7, 8); (b) effect of scalar field initial conditions ($\kappa_{max}\eta_B = 3.0$, cases 9, 10, 11).

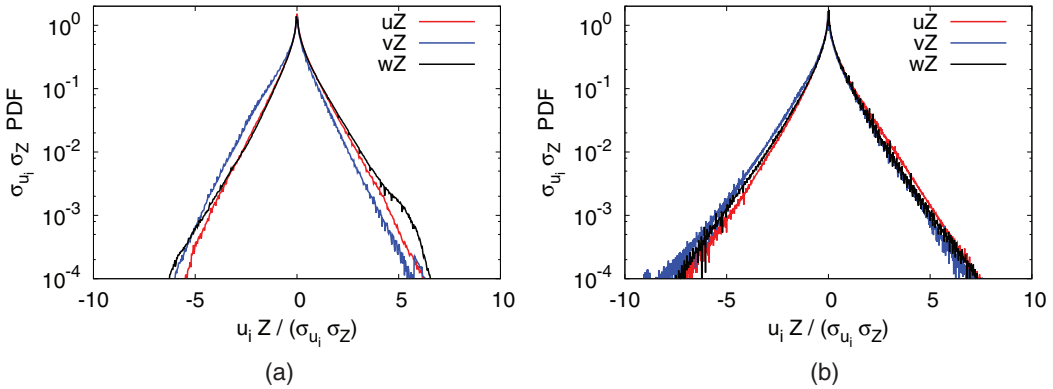

FIG. 8. PDF of scalar flux with the proposed linear scalar forcing for cases 1 and 3. (a) $Sc = 1$, $Re_\lambda = 55$; (b) $Sc = 16$, $Re_\lambda = 55$.

seed the simulation, consisting of random numbers bounded from −1 to 1 (case 10). Finally, the initial scalar field was taken to be a statistically stationary field obtained from implementing the mean scalar gradient forcing (case 11). The impact of these three different initial conditions on the behavior of the proposed forcing technique is depicted in Fig. 7(b). The proposed forcing technique successfully drives the scalar field to a constant variance regardless of its initial state.

The (potential) impact of the addition of the relaxation term in Eq. (18) on the long-term behavior of the scalar field has been investigated by considering different relaxation time-scales (Fig. 7(a)), initial fields (Fig. 7(b)), and different times (e.g., $t/\tau = 2$ and $t/\tau = 35$, Fig. 6). The statistics were found to be unchanged. As a result, it is believed that it is appropriate to conclude that the relaxation term included in Eq. (18) only drives the scalar variance to its desired value, having no adverse effects on the long-term statistics of the scalar field.

The statistical character of the scalar field under the action of the linear scalar forcing is found, also, to be favorable and approximately Gaussian, consistent with experimental findings. The skewness and flatness were calculated for each case included in the study. The skewness data indicated that the scalar field was symmetric about its mean (equally probable to have positive and negative scalar values), a requirement for homogeneous, isotropic turbulence. Additionally, the flatness of the scalar field was found to have a value of approximately three, consistent with that of a Gaussian distribution.

C. Single point scalar field statistics

To remain consistent with the physics of scalar mixing in a decaying turbulent field, the scalar statistics must be isotropic and symmetric. To determine if the proposed forcing is able to reproduce these requirements, the probability density functions of the three scalar fluxes for each simulation were calculated for cases 1–4. These cases correspond to moderate $Re_\lambda = 55$ conditions over a range of low to moderate $Sc = 0.5$, 1, 16 and one high $Re_\lambda = 140$ condition at $Sc = 1$. These scalar fluxes are averaged over multiple τ (eddy turn-over times) and two representative PDFs are depicted in Fig. 8. As is apparent in Fig. 8, the scalar fluxes are symmetrically distributed about a value of zero. Comparable distributions were found for all Re_λ and Sc examined in this study. This is in contrast to the strong anisotropy in the scalar fluxes obtained with the mean gradient forcing (Fig. 1).

The distribution of the scalar and scalar dissipation rate is also calculated. Under conditions of isotropy and homogeneity, the distribution of a scalar quantity is expected to be close to Gaussian, while that of the scalar dissipation rate is close to log-normal. The PDFs for these two quantities are included in Fig. 9. As shown in Fig. 9(a), the approximately Gaussian distribution of the scalar quantity, Z, is preserved with the proposed forcing. Additionally, Fig. 9(b) indicates that the commonly-accepted log-normal distribution of χ is preserved also under the action of the linear scalar forcing.

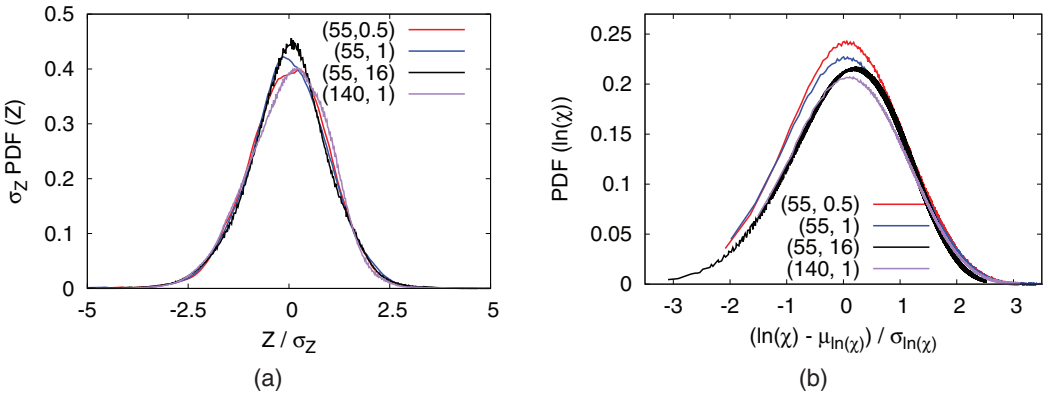

FIG. 9. PDF of scalar quantity, Z, and scalar dissipation rate, χ, with the proposed linear scalar forcing for cases 1–4. The legends refer to the (Re_λ, Sc) combination implemented. (a) Scalar field quantity, Z; (b) scalar dissipation rate, χ.

D. Two-point scalar field statistics

The final test is to ensure that the proposed scalar forcing reproduces adequately the scalar energy spectrum in the self-similar regime. Towards that end, a scalar field is forced via the mean gradient forcing from $t/\tau = -15$ until $t/\tau = 0$, after which it is allowed to decay. It is clear from Fig. 10(a) that after $t/\tau = 0$, the scalar variance decays in the absence of any external forcing. The analysis that follows focuses on the three data points depicted in Fig. 10(a), obtained 1, 4, and 7 τ after the beginning of decay, with the mean scalar gradient forcing term zeroed. The scalar spectra for these three data points are presented in Fig. 10(b), along with the spectrum obtained when the field was forced with a mean gradient, just prior to decay ($t/\tau = 0$). These spectra are not normalized, and they clearly indicate that the energy content of the scalar field is decreasing. However, the shape of the spectra are largely unchanged, suggesting a possible self-similar behavior. To verify that the scalar field had entered a self-similar state, the spectra at 1, 4, and 7 τ after the onset of variance decay were suitably normalized by their Batchelor scales and their variances, σ_Z^2. The results are displayed in Fig. 10(c). The collapse of the spectra to one consistent curve for two of the three data points ($t/\tau = 4$ and 7) confirms that the scalar field has entered into a self-similar regime. The scalar dissipation spectra, defined as $D(\kappa) = \mathcal{D}\kappa^2 E(\kappa)$, are presented in the inset to highlight this collapse. As shown in the dissipation spectra comparison, the data at $t/\tau = 1$ does not collapse on to the same spectrum as the other two, indicating that this data point is located in the transient period between statistical stationarity and self-similar behavior. The number of eddy turn-over times (τ) of decay needed for the scalar field to enter into the self-similar regime varies with Re_λ and Sc; in all cases included in this study, it was verified that sufficient time had passed to allow for the self-similar regime to develop fully.

To prove that the linear scalar forcing produces the physics of self-similar decay, the decaying spectra that have entered the self-similar regime, such as those in Fig. 10(c), are compared to the scalar spectrum obtained when a scalar field is forced via the linear scalar forcing method. Representative results are depicted in Fig. 10(d). Collapse of the normalized decaying spectra onto the spectrum predicted by the linear scalar forcing confirms that the proposed forcing does reproduce accurately the physics of scalar mixing in the self-similar regime. For clarity, only one of the three decaying spectra, at $t/\tau = 7$, is used for the comparison to the linearly-forced scalar spectrum, although spectra at $t/\tau = 4$ and 7 exhibit the same behavior.

The preceding analysis focused on case 1 in Table I, where the Schmidt number was unity. To confirm that this behavior persisted for non-unity Sc and other Re_λ, the same analysis was conducted using cases 2–5. In all cases, the freely decaying spectra assumed the spectrum shape predicted by the linear scalar forcing method. Taking as examples the two extreme Sc included in this study ($Sc = 0.5$ and $Sc = 256$), Fig. 11 details the self-similar collapse of freely-decaying spectra onto the spectrum shape predicted by the linear scalar forcing. The extent of agreement between the decaying and linearly-forced scalar spectra is highlighted in Figs. 11(c) and 11(d), which displays the dissipation

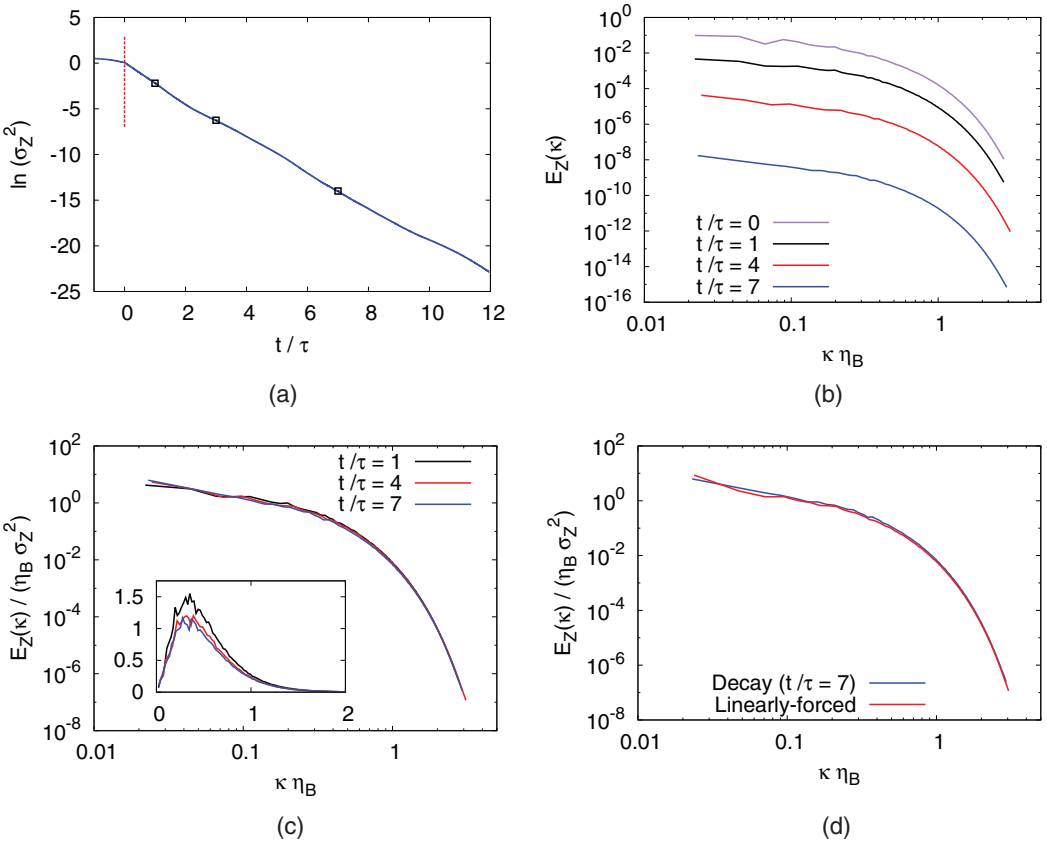

FIG. 10. Evolution of a purely decaying scalar spectrum into the shape predicted by the proposed linear scalar forcing method ($Re_\lambda = 55$, $Sc = 1$, case 1). (a) Decay of scalar variance. Points correspond to scalar variance 1, 4, and 7 τ after forcing is removed; (b) scalar spectra in self-similar regime; (c) collapse of normalized scalar spectra. The inset is the dissipation spectrum, $10^2 \times D(\kappa)$; (d) collapse of normalized scalar spectra in the self-similar regime.

spectra for the two cases. As is apparent, the linear scalar forcing predicts the appropriate spectrum of a decaying scalar. This behavior was observed for all cases included in this study and persisted irrespective of the initial conditions implemented.

V. IMPLICATIONS FOR HIGH-SCHMIDT NUMBER SCALAR MIXING

The mean gradient and linear scalar forcings are intended to capture two distinctly different scalar field physics. This difference manifests in the structure of the scalar spectra that the two methods predict. The stationary scalar spectra generated by the two techniques are provided in Fig. 11 for the lowest and highest Schmidt numbers investigated ($Sc = 0.5,\ 256$). Comparing these spectra, it is clear that continuous energy injection (mean gradient forcing) and one-time energy injection (linear scalar forcing) can predict different scalar field structures under certain conditions.

The simulation results for small Sc are considered first (Figs. 11(a) and 11(c)). At $Sc < 1$, the spectrum predicted by the two forcing methods are comparable. However, at $Sc \gg 1$ (Figs. 11(b) and 11(d)), there are distinct differences in shape (the distribution of scalar variance in wavespace) observable between the scalar spectra generated under mean gradient and linear scalar forcing. The mean gradient-predicted spectrum decays less strongly across the intermediate wavenumbers than that predicted by the proposed forcing method. These differences are more pronounced at larger Sc and can be considered in terms of Batchelor's theory for scalar behavior[19] and experimentally-observed high-Schmidt number scalar behavior.[20–23]

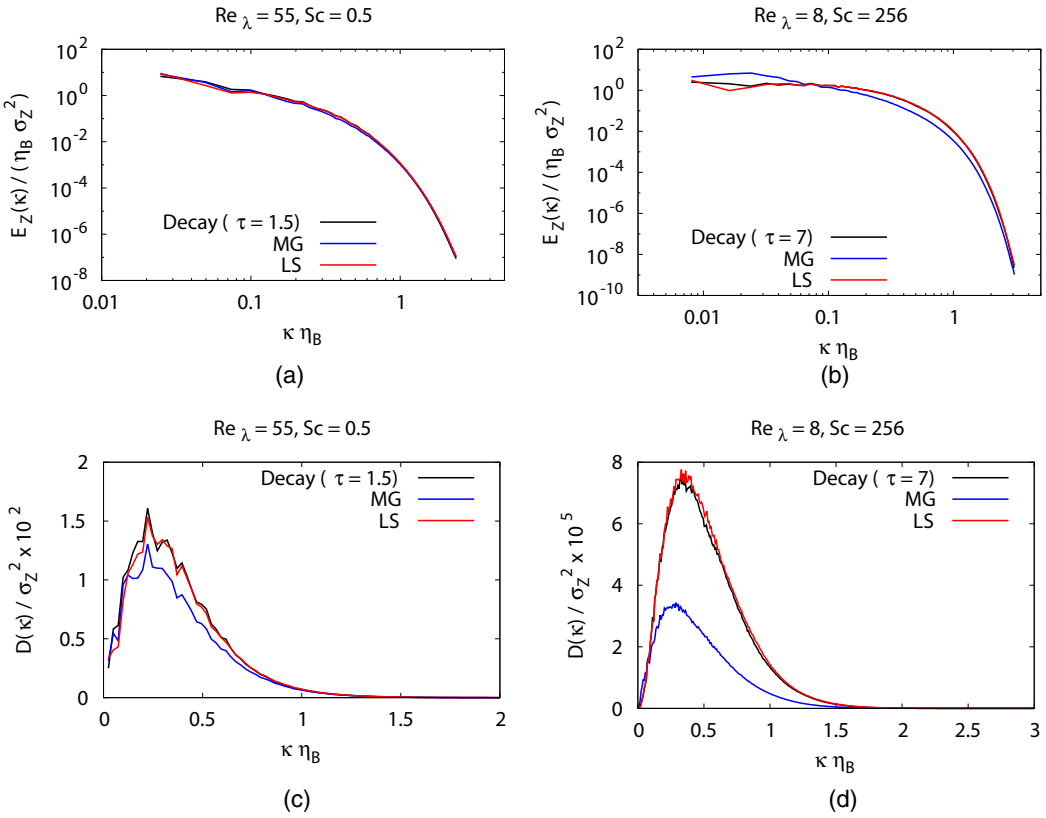

FIG. 11. Evolution of a purely decaying scalar spectrum into the shape predicted by the proposed linear scalar forcing method. Linear scalar and mean gradient forcing are denoted as LS and MG. (a) Collapse of decaying spectra onto linear scalar forcing-predicted shape; (b) collapse of decaying spectra onto linear scalar forcing-predicted shape; (c) comparison of freely decaying and linear scalar forcing-predicted dissipation spectra; (d) comparison of freely decaying and linear scalar forcing-predicted dissipation spectra.

Batchelor's theory predicts that the scalar energy spectrum will present distinct regions in wavenumber space with distinct scalings; the emergence of these regions is dependent on the Schmidt number of the scalar.[19] For high Schmidt number scalars ($Sc \gg 1$), there are two characteristic regions. The first is the inertial-convective subrange, which manifests at scales larger than the Kolmogorov scale. The second is the viscous-convective subrange, which is present for scales, l, bounded between the Kolmogorov and Batchelor[19] scales, $\eta \ll l \ll \eta_B$. The scalar energy spectrum ($E_Z(\kappa)$) in the inertial-convective and viscous-convective subranges is predicted, further, to scale according to $\kappa^{-5/3}$ (for sufficiently high Reynolds numbers)[24] and κ^{-1} (irrespective of the Reynolds number), respectively, where κ is the wavenumber.[19] It is the scaling in the viscous-convective region with which the present analysis is concerned. In contradiction to Batchelor's[19] prediction, several experimental studies of high Schmidt number turbulent scalars have not observed the κ^{-1} scaling behavior.[20–23] Some observed that a weaker scaling, possibly a log-normal scaling, across the viscous-convective subrange may be more representative of experimental data.[20]

Case 5 has a sufficiently high $Sc = 256$ to allow for a comparison of the scalar spectra produced by the linear scalar and mean gradient forcing methods to both Batchelor's[19] predictions and the summarized experimental results. As the Reynolds number is low ($Re_\lambda \approx 8$), it is not expected to capture the $\kappa^{-5/3}$ scaling across the inertial-convective range as predicted by Obukhov[25] and Corrsin,[24] but it is expected that the Schmidt number is high enough to capture the correct behavior across the viscous-convective range. To compare the data presented to Batchelor's[19] scaling prediction, the Kraichnan[26] model spectrum (K-form) will be used. The Kraichnan spectrum introduces into

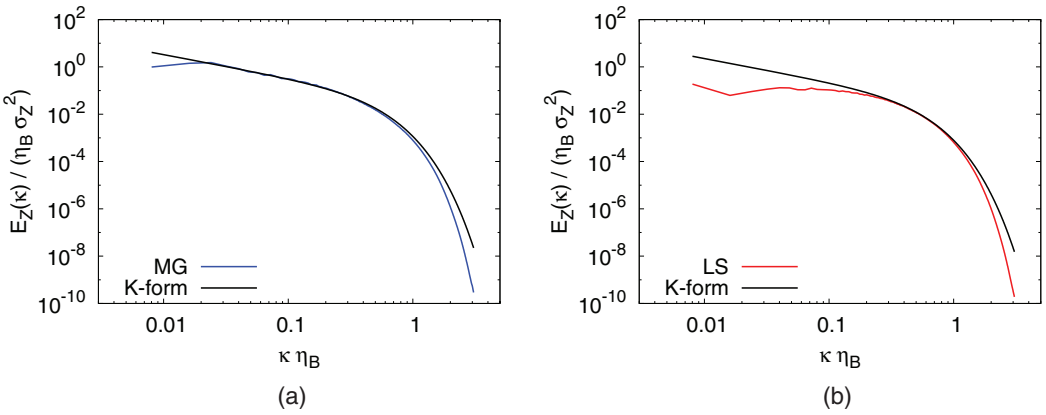

FIG. 12. Comparison of predicted scalar spectra to Kraichnan-predicted[26] form ($Re_\lambda = 8$, $Sc = 256$). The Batchelor[19] and Kraichnan[26] predicted scaling of $E_Z(\kappa) \propto \kappa^{-1}$ is represented by the Kraichnan[26] model spectrum (black). Note the Kraichnan[26] spectra have been shifted slightly vertically to highlight consistency (or inconsistency) with the MG and LS spectra. (a) Mean gradient-forced spectra; (b) linear scalar-forced spectra.

Batchelor's[19] proposed spectrum form a correction allowing for fluctuations in strain rate.[26] This model form was obtained strictly theoretically, and it is given by

$$E_Z(\kappa) = q\langle\chi\rangle \left(\frac{\nu}{\epsilon}\right)^{-1/2} \kappa^{-1} \left(1 + \kappa\eta_B\sqrt{6q}\right) \exp\left(-\kappa\eta_B\sqrt{6q}\right), \tag{19}$$

where q was determined by Qian to have a value of $2\sqrt{5}$ for homogeneous, isotropic turbulence.[27] One of the assumptions made by both Batchelor[19] and Kraichnan[26] was that the scalar field is subject to continuous scalar variance injection (infinite scalar reservoir). The presence of an infinite reservoir of variance will produce a scalar energy distribution that is distinct, and this is the distribution that the mean gradient forcing was developed to capture.

To emphasize the differences between the mean gradient and linear scalar forcing techniques, they are compared directly to the K-form model spectrum. Figure 12(a) compares the statistically stationary scalar spectrum predicted by the mean gradient forcing to Kraichnan's[26] model. As is apparent in Fig. 12(a), the mean gradient spectrum agrees quite well with the K-form spectrum. Alternatively, the linear forcing assumes one-time scalar variance injection, contrary to the explicit assumptions of the K-form spectrum. Unsurprisingly, Fig. 12(b), which compares Kraichnan's[26] model to the spectrum predicted by the linear scalar forcing, finds virtually no agreement. Note for the mean scalar gradient forcing that the disagreement in the viscous-diffusive subrange between the K-form and predicted spectrum can be attributed to numerical losses, which have minimal negative impact in the viscous-convective subrange.

As is evident from Fig. 12, the scalar spectra resulting from the two different scalar forcing techniques exhibit different scaling behaviors across the viscous-convective subrange. The mean scalar gradient forcing appears to obey the κ^{-1} scaling, while the proposed scalar forcing does not. In fact, the proposed scalar forcing implies a scaling with wavenumber that is weaker than κ^{-1}, possibly consistent with experimental findings. The difference between the physics corresponding to the two scalar forcing techniques could provide insight into the apparent disagreement between the experimental results and theoretical analysis in the literature. The presence of a constant, uniform mean scalar gradient is more consistent with the assumptions used in the derivation of Batchelor's[19] theoretical scaling, namely, the assumption of an infinite scalar reservoir. On the other hand, the self-similar nature of scalar mixing in decaying turbulence might be more consistent with experimental observations, as they both are limited to having only a finite, initial scalar variance distribution. Stated differently, the apparent disagreement between experiments and theory could be due only to the conditions under which scalar mixing is considered, whether that be in a decaying, self-similar (appropriate for experiments) or forced (appropriate for Batchelor's[19] predictions) scalar field. This warrants additional investigation. However, this is beyond the scope of the present study.

VI. CONCLUSIONS

The primary objective of this work was to develop a methodology for numerically simulating the self-similar decay of a turbulent scalar field. The linear scalar forcing technique has been presented and the statistics produced by its implementation have been shown to reproduce the characteristics of homogeneous, isotropic turbulence. For the range of Sc considered in this study, the spectra predicted by the proposed scalar forcing are consistent with the sustained decay of a turbulent scalar field. The proposed forcing is robust, performing well irrespective of the initial conditions of the flow field.

The proposed scalar forcing is both novel and attractive relative to the most commonly-used scalar forcings (mean scalar gradient and spectral). Spectral schemes require periodic boundaries, are, in general, memory and computationally intensive, and impose constraints that are not easily realizable in experiments. In comparison, the linear scalar forcing can accommodate non-periodic boundary conditions, which are almost always needed when modeling engineering problems, and can be integrated easily into non-spectral (physical) codes. Compared to the mean gradient forcing, the proposed linear scalar forcing will be slightly more memory intensive, as it requires storage and calculation of the scalar field variance and scalar dissipation rate at each timestep. However, this is not a significant increase.

Finally, it has been suggested that the proposed linear scalar forcing may provide insight into the nature of high Schmidt number flows. Specifically, the disparity observed between the scalar energy spectra generated by the well-established mean scalar gradient and the proposed linear forcing are reminiscent of the observed differences between theoretical predictions and experimental results. These differences may be simply a consequence of the conditions under which scalar mixing is studied. The implementation of a mean scalar gradient corresponds to a scalar field with continuous energy injection, while the proposed linear scalar forcing simulates sustained decay of scalar variance. As presented, this methodology can be implemented to perform simulation studies of the mixing of passive scalar quantities in a turbulent environment.

ACKNOWLEDGMENTS

This work used the Extreme Science and Engineering Discovery Environment (XSEDE), which is supported by National Science Foundation Grant No. OCI-1053575. This research was supported by the National Science Foundation CAREER award Grant No. 1056142. Also, the authors would like to acknowledge Adam Cheminet (ONERA), whose contribution was integral in the early stages of this study.

[1] P. K. Yeung, "Schmidt number effects on turbulent transport with uniform mean scalar gradient," Phys. Fluids **14**, 4178 (2002).
[2] D. A. Donzis, K. R. Sreenivasan, and P. K. Yeung, "The Batchelor spectrum for mixing of passive scalars in isotropic turbulence," Flow, Turbul. Combust. **85**, 549 (2010).
[3] R. M. Kerr, "Higher-order derivative correlations and the alignment of small-scale structures in isotropic numerical turbulence," J. Fluid Mech. **153**, 31 (1985).
[4] T. Gotoh and T. Watanabe, "Scalar flux in a uniform mean scalar gradient in homogeneous isotropic steady turbulence," Physica D **241**, 141 (2012).
[5] D. A. Donzis, K. R. Sreenivasan, and P. K. Yeung, "Scalar dissipation rate and dissipative anamoly in isotropic turbulence," J. Fluid Mech. **532**, 199 (2005).
[6] T. S. Lundgren, "Linearly forced isotropic turbulence," in *Annual Research Briefs* (Center for Turbulence Research, Stanford, 2003), pp. 461–473.
[7] C. Rosales and C. Meneveau, "Linear forcing in numerical simulations of isotropic turbulence: Physical space implementations and convergence properties," Phys. Fluids **17**, 095106 (2005).
[8] Z. Warhaft, "Passive scalars in turbulent flows," Annu. Rev. Fluid Mech. **32**, 203 (2000).
[9] T. Watanabe and T. Gotoh, "Intermittency in passive scalar turbulence under the uniform mean scalar gradient," Phys. Fluids **18**, 058105 (2006).
[10] K. Alvelius, "Random forcing of three-dimensional homogeneous turbulence," Phys. Fluids **11**, 1880 (1999).
[11] S. Chen and N. Cao, "Anomalous scaling and structure instability in three-dimensional passive scalar turbulence," Phys. Rev. Lett. **78**, 3459 (1997).
[12] T. Watanabe and T. Gotoh, "Statistics of a passive scalar in homogeneous turbulence," New J. Phys. **6**, 40 (2004).
[13] X. Liu, S. Osher, and T. Chan, "Weighted essentially non-oscillatory schemes," J. Comput. Phys. **115**, 200 (1994).

[14] R. Nourgaliev and T. Theofanous, "High-fidelity interface tracking in compressible flows: Unlimited anchored adaptive level set," J. Comput. Phys. **224**, 836 (2007).
[15] B. P. Leonard, "A stable and accurate convective modelling procedure based on quadratic upstream interpolation," Comput. Methods Appl. Mech. Eng. **19**, 59 (1979).
[16] P. K. Yeung, S. Xu, D. A. Donzis, and K. R. Sreenivasan, "Simulations of three-dimensional turbulent mixing for Schmidt numbers of the order 1000," Flow, Turbul. Combust. **72**, 333 (2004).
[17] O. Desjardins, G. Blanquart, G. Balarac, and H. Pitsch, "High order conservative finite difference scheme for variable density low Mach number turbulent flows," J. Comput. Phys. **227**, 7125 (2008).
[18] V. Eswaran and S. B. Pope, "An examination of forcing in direct numerical simulations of turbulence," Comput. Fluids **16**, 257 (1988).
[19] G. K. Batchelor, "Small-scale variation of convected quantities like temperature in turbulent fluid. Part 1: General discussion and the case of small conductivity," J. Fluid Mech. **5**, 113 (1959).
[20] P. L. Miller and P. E. Dimotakis, "Measurements of scalar power spectra in high Schmidt number turbulent jets," J. Fluid Mech. **308**, 129 (1996).
[21] A. E. Gargett, "Evolution of scalar spectra with the decay of turbulence in a stratified fluid," J. Fluid Mech. **159**, 379 (1985).
[22] S. Komori, T. Kanzaki, Y. Murakami, and H. Ueda, "Simultaneous measurements of instantaneous concentrations of two species being mixed in a turbulent flow by using a combined laser-induced fluorescence and laser-scattering technique," Phys. Fluids A **1**, 349 (1989).
[23] P. L. Miller and P. E. Dimotakis, "Stochastic geometric properties of scalar interfaces in turbulent jets," Phys. Fluids A **3**, 168 (1991).
[24] S. Corrsin, "On the spectrum of isotropic temperature fluctuations in an isotropic turbulence," J. Appl. Phys. **22**, 469 (1951).
[25] A. M. Obukhov, "Structure of the temperature field in a turbulent flow," Izv. Akad. Nauk. SSSR, Ser. Geogr. Geofiz. **13**, 58 (1949).
[26] R. H. Kraichnan, "Small-scale structure of a scalar field convected by turbulence," Phys. Fluids **11**, 945 (1968).
[27] J. Qian, "Viscous range of turbulent scalar of large Prandtl number," Fluid Dyn. Res. **15**, 103 (1995).